

Adsorption of Anionic and Cationic Dyes Using Functionalized ZnCl₂-Activated Charcoal Derived from Coconut Shells

Kamiludeen OLANREWAJU^{1,2}, Kamoru A. SALAM³, Abdullahi M. EVUTI⁴, Abdulwasiu ABDURRAHMAN⁵

¹Department of Nuclear Engineering, Faculty of Engineering, University of Abuja, Abuja, Nigeria

^{2,3,4,5}Department of Chemical Engineering, Faculty of Engineering, University of Abuja, Abuja, Nigeria

^{1,2}kamiludeen.olarenwaju@uniabuja.edu.ng, ³kamorusalam@gmail.com, ⁴mohammed.evuti@uniabuja.edu.ng,
⁵abdulwasiu.abdurrahman@uniabuja.edu.ng

Abstract

Synthetic dyes, both cationic and anionic, are among the primary pollutants impacting aquatic systems. This work explores the adsorption performance of nitric acid-modified ZnCl₂-activated carbon obtained from coconut shells for the elimination of Methylene Blue (MB) and Congo Red (CR) dyes from water. The adsorbent was characterized using Fourier Transform Infrared (FTIR) spectroscopy and Brunauer–Emmett–Teller (BET) surface area analysis. Batch adsorption tests were carried out to determine the effects of contact time, initial dye concentration, adsorbent dosage, and pH on dye removal efficiency. Equilibrium was reached within 30 minutes, and the adsorption data fit both Langmuir and Freundlich models, with the Langmuir isotherm providing a slightly better correlation. Activation of the ordinary carbonised coconut shell (OCCNS) with phosphoric acid increases its specific surface area from 135.5 to 435.98m²/g and pore volume from 0.055 to 0.154cm³/g. Post treatment of the activated charcoal with nitric acid further increases its specific surface area to 810.44m²/g and pore volume of 0.296cm³/g which improves the adsorption capacity of the adsorbents. Surface modification significantly enhanced both the surface area and adsorption capacity; the highest monolayer adsorption capacities for MB and CR were 6.33 mg/g and 7.04 mg/g, correspondingly. The functionalized activated carbon showed high potential as a cost-effective and environmentally sustainable adsorbent for the purification of dye-laden wastewater due to its amphoteric surface behavior.

Keywords: Activated charcoal, Adsorption, Congo red, Functionalization, Methylene blue.

1.0 Introduction

Industrial effluents containing dyes from textile, leather, food, cosmetic, paper, rubber, and plastic industries have emerged as major environmental pollutants because of their durability, toxicity, and resistance to biodegradation (Ahmad et al., 2025; Ait et al., 2018). These sectors consume substantial volumes of water and release large quantities of intensely colored wastewater into aquatic systems. Such effluents disrupt aquatic ecosystems by reducing light penetration, inhibiting photosynthesis, and introducing carcinogenic or mutagenic substances (González-García et al., 2022). Consequently, the development of efficient, economical, and sustainable dye-removal strategies has become a crucial focus in environmental and wastewater management.

Due to their deliberate chemical stability, synthetic dyes resist oxidation, heat, and microbial degradation (Hu et al., 2016). Once discharged into the environment, they persist for long periods and are difficult to decompose, necessitating efficient treatment methods. A broad spectrum of physicochemical and biological techniques – such as ion exchange, precipitation, reverse osmosis, and adsorption – have been used for dye removal. Among these, adsorption stands out for its operational simplicity, affordability, and high removal efficiency (Hayfron et al., 2025; Homagai et al., 2022; Lawtae & Tangsathitkulchai, 2021). Activated carbon remains the most widely employed adsorbent owing to its high porosity, extensive surface area, and superior adsorption properties (Gupta et al., 2020; Hasanzadeh et al., 2020). However, large-scale utilization is restricted by high production costs. This has encouraged research into alternative low-cost, renewable adsorbents derived from agricultural and biological wastes. The precursor and activation process greatly influence the final structure and surface chemistry of activated carbon (Suzuki, 1994; Tadda et al., 2016). Various plant-based materials such as rice husks, bamboo, maize stalks, pomegranate peels, olive stones, and coconut shells have been explored for activated carbon synthesis (Heidarinejad et al., 2020; Manoj et al., 2021).

Among these biomaterials, coconut shells are particularly promising because of their high carbon yield, abundance, and renewability (Hasanzadeh et al., 2020). The adsorption capability of coconut-shell-based activated carbon for dye removal has been widely validated. For example, Zhou et al. (2018) reported

that shrimp-shell-based carbon achieved a capacity of 288.2 mg g^{-1} for Congo Red removal, whereas Ahmad & Kumar (2010) recorded 98.03 mg g^{-1} for Bael shell-derived carbon. Similarly, nano-activated carbon synthesized from industrial mining coal demonstrated excellent efficiency for methylene blue removal (Shokry *et al.*, 2019).

Chemical surface modification can further improve adsorption characteristics. Nitric acid oxidation introduces oxygen-rich functional groups that increase polarity and strengthen electrostatic interaction with both positively and negatively charged dye molecules (Allwar *et al.*, 2017). Despite many advances, most previous works have focused on single dye systems, whereas actual industrial wastewater usually contains mixed ionic dyes. This underscores the need for multifunctional adsorbents capable of removing diverse dye species simultaneously.

This study investigates the adsorption potential of nitric-acid-treated ZnCl_2 -activated carbon synthesized from coconut shells for the simultaneous removal of Congo Red (anionic) and Methylene Blue (cationic) dyes. The adsorbent was analyzed using BET and FTIR techniques, and the equilibrium data were interpreted through Langmuir and Freundlich models to determine adsorption mechanisms. The findings are expected to contribute to developing cost-efficient, environmentally friendly adsorbents for industrial wastewater treatment.

2.0 Materials and Methods

2.1 Materials

All reagents utilized in this work were of analytical grade. The dyes—Methylene Blue (MB) and Congo Red (CR)—were sourced from Sigma-Aldrich and used without further purification. Nitric acid (65%) and sodium hydroxide (97%) were obtained from Planlac Nigeria Enterprise, Minna. Figures 1 and 2 illustrate the molecular structures and properties of MB and CR. Locally collected coconut shells were thoroughly washed with distilled water and oven-dried to constant weight prior to use in adsorbent preparation.

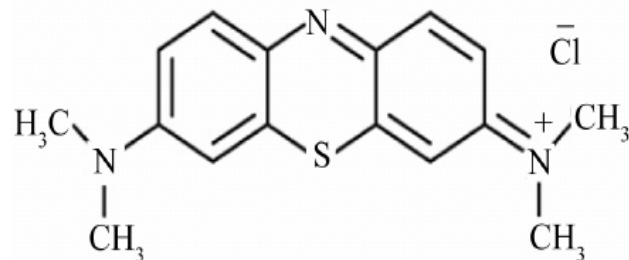


Figure 1: Chemical structure of Methylene Blue (MB), $M_w = 319.9 \text{ g/mol}$, $\lambda_{max} = 670 \text{ nm}$

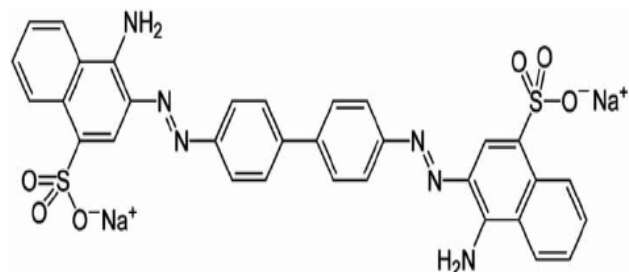


Figure 2: Chemical structure of Congo Red (CR), $M_w = 696.7 \text{ g/mol}$, $\lambda_{max} = 488 \text{ nm}$

2.1 Preparation of Activated Charcoal

Activated carbon was synthesized from coconut shell powder through sequential stages of pre-treatment, chemical impregnation with zinc chloride, carbonization, leaching, and nitric acid functionalization.

2.2 Preparation of the Coconut shells

Coconut shells were obtained from vendors at Suleja, Niger State. They were cleaned with distilled water to eliminate impurities and sun-dried for 8–10 hours. The dried shells were manually crushed and ground into fine powder using a local milling machine. The powder was sieved, and particles smaller than $150 \mu\text{m}$ were selected for subsequent activation.

2.3 Impregnation and carbonization with zinc chloride

A measured quantity (200 g) of the sieved coconut shell powder was mixed with concentrated $ZnCl_2$ solution (98% anhydrous). About 100 g of this impregnated material was soaked in one liter of distilled water for one hour, filtered, and dried at 60°C for 12 hours. The dried sample was then carbonized at 750°C for one hour in a muffle furnace.

After cooling, the carbonized product was treated with 1 M HCl solution at 80°C for 24 hours to remove residual zinc chloride. The mixture was thoroughly washed with distilled water until the filtrate no longer contain any traces of chloride ions, confirmed via silver nitrate test. The sample was then oven-dried at 110°C for two hours to determine the yield of activated carbon (Lawal *et al.* 2018).

$$\% \text{ yield} = \frac{W_a}{W_p} \times 100 \quad (1)$$

Where W_a is the weight of activated charcoal
 W_p is the weight of precursor

2.4 Functionalization of the activated charcoal

2.4.1 Oxidation with Nitric Acid

10 g of the activated carbon were soaked in 100 cm³ of 2 M nitric acid solution for 24 hours. After acid treatment, the material was washed repeatedly with distilled water to remove residual acid and dried at 120°C. The nitric acid-modified activated carbon was then stored in airtight containers for later use.

2.5 Preparation of Dyestuff

A stock solution of each dye was prepared by dissolving 1 g of Methylene Blue or Congo Red in 1 L of distilled water. Working solutions of different concentrations (10, 40, 60, 80, and 120 mg/L) were prepared by appropriate dilution from the stock.

2.6 Batch Adsorption Experiments

Adsorption experiments were conducted by agitating 50 mL of dye solution of desired concentration with the required adsorbent dosage in 100 mL beakers at 150 rpm. The influence of contact time (10–60 min), starting dye concentration (10–120 mg/L), adsorbent dosage (0.5–3 g), and pH (2–12) was examined. The pH of the solution was modified using 0.1 N NaOH or 0.1 N HNO_3 and measured with a calibrated pH meter. Temperature was maintained using a thermostatically controlled incubator.

After adsorption, the samples were centrifuged at 3000 rpm for 10 minutes to separate the solid and liquid phases. The residual dye concentration was determined spectrophotometrically at the dyes' respective maximum wavelengths (Figures 1 and 2). The adsorption capacity was calculated using Equation (2):

$$q_m = \frac{(C_i - C_f)V}{m} \quad (2)$$

Where

C_i (mg/L) is the starting dye concentration

q_m (mg/g) is the adsorbed quantity.

The mass of the adsorbent is denoted by m (g),

whereas the dye concentration at a given time is represented by C_f (mg/L).

3.0 Results and Discussion

3.1 Characterization of the Adsorbent

3.1.1 FTIR Analysis

Figure 3 displays the FTIR spectra of the carbonized, $ZnCl_2$ -activated, and nitric acid-modified activated carbons derived from coconut shells. Four major absorption peaks were observed at approximately 2916 cm⁻¹, 2833 cm⁻¹, 1666–1708 cm⁻¹, and 1375–1458 cm⁻¹. Peaks near 2916 cm⁻¹ and 2833 cm⁻¹ correspond to C-H stretching vibrations, whereas those around 1666–1708 cm⁻¹ indicate carbonyl (C=O) stretching ("Interpretation of Infrared Spectra, A Practical Approach," 2000). The bands within 1375–1458 cm⁻¹ are attributed to C-H bending of methyl and methylene functional groups (Punyani *et al.*, 2006).

Comparison of the spectra reveals that nitric acid treatment did not introduce new functional groups but enhanced the intensity of existing oxygen-containing ones, confirming successful surface oxidation. The increased peak intensity suggests a higher abundance of oxygenated sites that promote stronger dye-surface interactions. Additionally, the presence of aromatic units (benzene rings) facilitates π - π stacking between the dye molecules and carbon surface, improving adsorption performance. Thus, both surface chemistry and structure contribute significantly to adsorption efficiency.

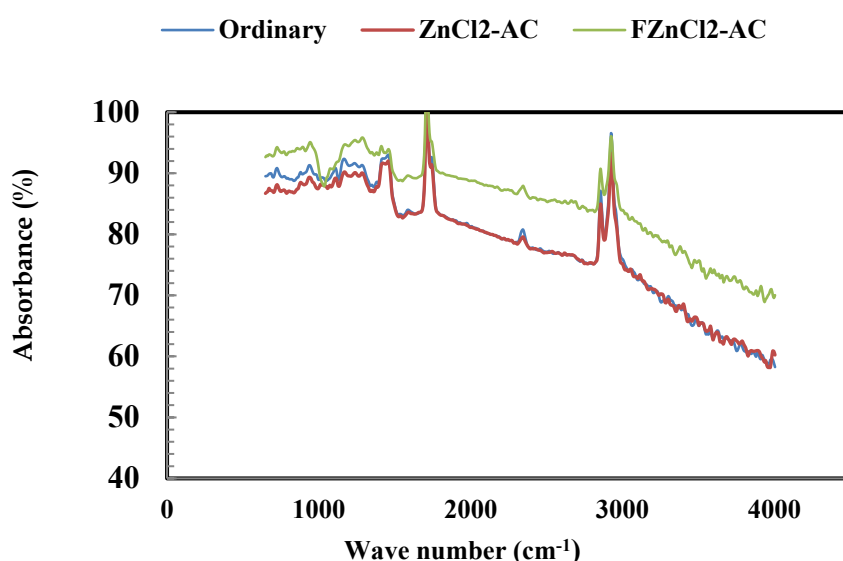


Figure 3: FTIR spectra of carbonized, ZnCl_2 -activated, and nitric acid-functionalized activated carbons.

3.1.2 BET Surface Area and Pore Volume Analysis

BET analysis revealed that the specific surface areas of ordinary carbon (OCCNS), ZnCl_2 -activated carbon (ZAC), and nitric acid-modified activated carbon (FZAC) were $135.55 \text{ m}^2/\text{g}$, $435.98 \text{ m}^2/\text{g}$, and $810.44 \text{ m}^2/\text{g}$, respectively (Figure 4). Nitric acid treatment notably increased the surface area and pore volume (Figure 5), signifying improved porosity and accessibility of adsorption sites.

The rise in both parameters indicates that activation and acid treatment effectively removed volatile matter and created a more developed pore structure. These findings concur with those of Allwar *et al.* (2017), who found that acid functionalization enhances porosity and adsorption potential in carbon materials. Consequently, the structural development observed in FZAC accounts for its superior adsorption efficiency toward both Congo Red (CR) and Methylene Blue (MB).

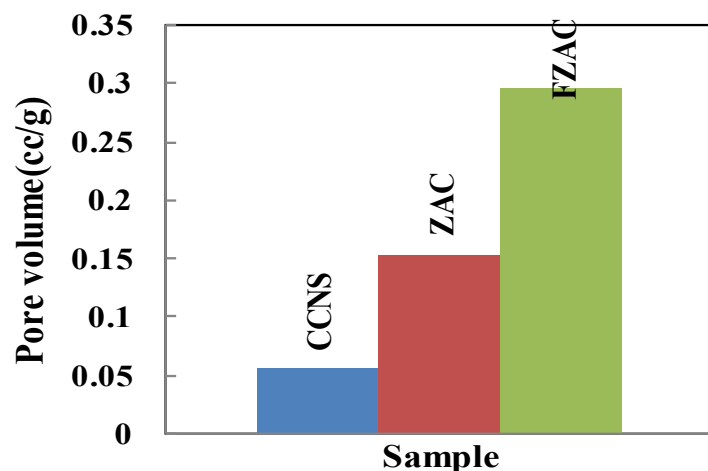


Figure 4: Specific surface areas of non-activated, activated, and functionalized carbons.

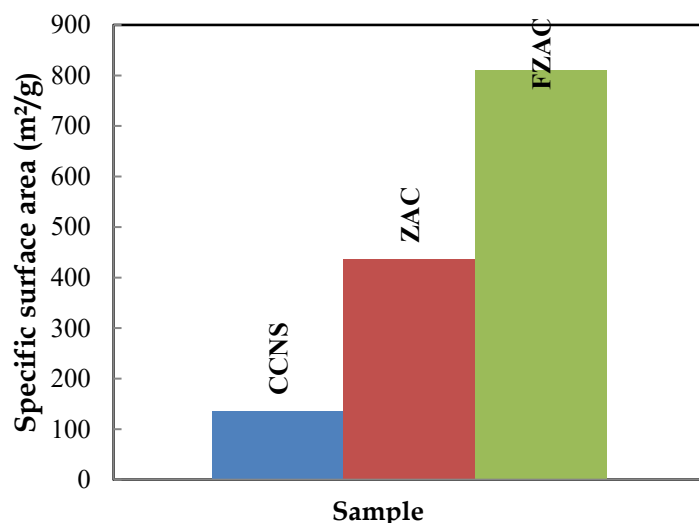


Figure 5: Pore volumes of non-activated, activated, and functionalized carbons.

3.2 Adsorption Behaviour

The adsorption kinetics of Methylene Blue and Congo Red were evaluated using both unmodified (UZAC) and nitric acid-functionalized (FZAC) ZnCl_2 -activated carbons. Parameters such as contact time, solution pH, adsorbent dosage, and initial dye concentration were investigated to determine optimal conditions.

3.2.1 Impact of contact duration

Adsorption of both dyes increased rapidly during the first 10 minutes and reached equilibrium at about 30 minutes (Figure 6). The initial fast phase is due to the abundance of active sites, followed by slower adsorption as sites become saturated. Beyond 30 minutes, no significant improvement was observed, indicating equilibrium.

The equilibrium time is consistent with prior studies, which reported 30–40 minutes for similar dye-carbon systems (Mohammed *et al.*, 2014; Wan Ibrahim *et al.*, 2019; Yakubu *et al.*, 2024). The faster equilibrium observed for FZAC reflects improved porosity and surface accessibility resulting from nitric acid modification.

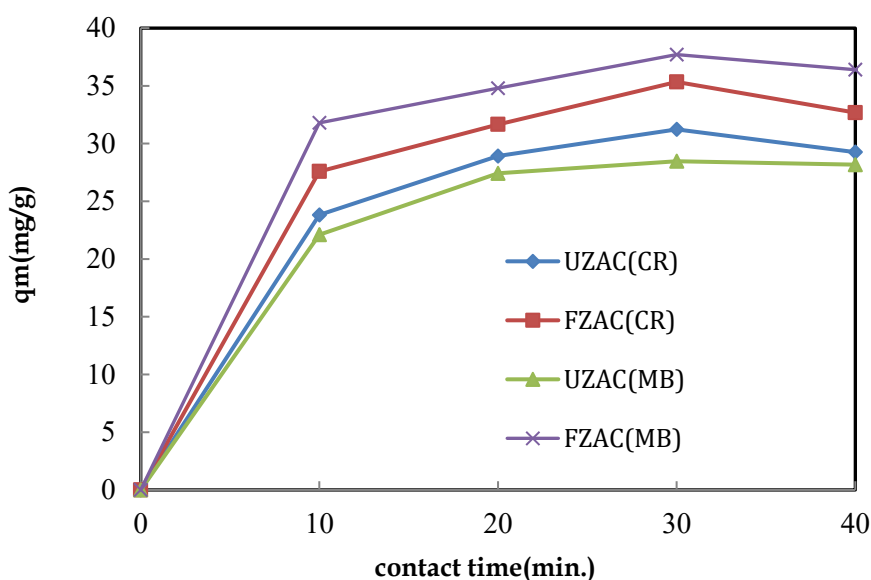


Figure 6: Effect of contact time on MB and CR adsorption by UZAC and FZAC.

3.2.2 Effect of pH

Solution pH strongly affected the adsorption of both dyes (Figure 7). As pH increased, MB adsorption improved, while CR removal decreased. At low pH, the carbon surface becomes positively charged, favoring

adsorption of anionic CR molecules but repelling cationic MB ions. At higher pH, the surface becomes negatively charged, enhancing MB adsorption but reducing CR uptake. This amphoteric nature implies that the adsorbent's surface charge varies with pH, enabling it to capture both dye types under appropriate conditions (Ai *et al.*, 2011; Yakubu *et al.*, 2024).

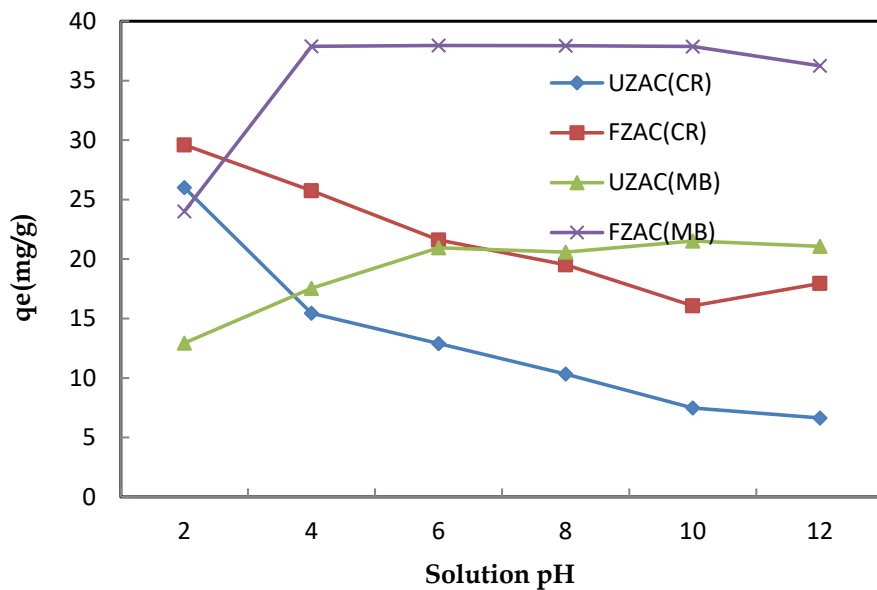


Figure 7: Effect of solution pH on MB and CR adsorption by UZAC and FZAC.

3.2.3 Impact of adsorbent dosage

Increasing the adsorbent dosage from 0.5 g to 3 g improved dye removal for both MB and CR (Figure 8). The FZAC achieved removal efficiencies of 99.5% (MB) and 91% (CR), whereas UZAC showed slightly lower values. The improvement is attributed to a higher number of available adsorption sites and greater surface area.

The better performance of FZAC highlights the beneficial effect of nitric acid treatment in improving surface chemistry and porosity. Comparable findings have been documented by Bai (2001), Barka *et al.* (2013), and Cayllahua *et al.* (2009).

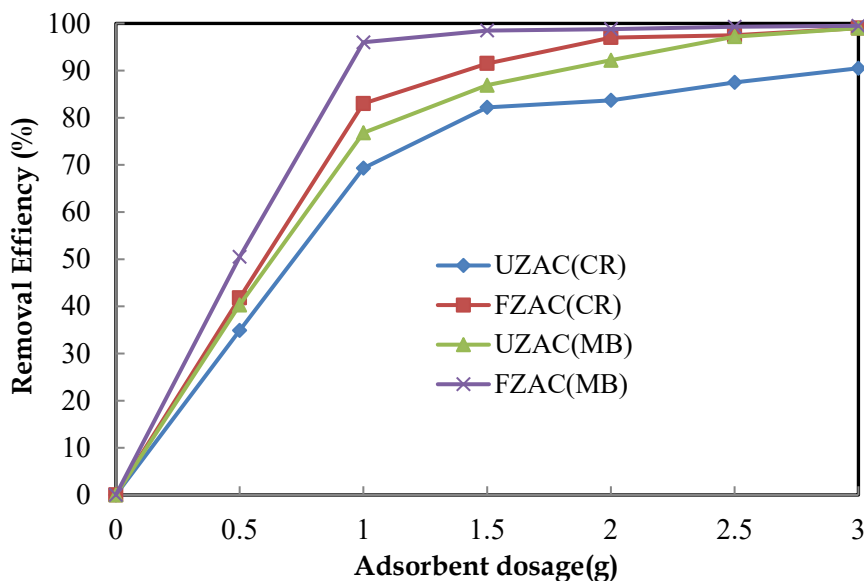


Figure 8: Effect of adsorbent dosage on MB and CR adsorption by UZAC and FZAC.

3.2.4 Effect of initial dye concentration

As depicted in Figure 9, adsorption capacity increased with higher initial dye concentration, owing to an increased driving force for mass transfer. For MB, capacity rose from 0 to 37.8 mg/g for FZAC and from 0 to 31.3 mg/g for UZAC, while CR rose from 0 to 32.6 mg/g (FZAC) and 0 to 26.7 mg/g (UZAC).

The higher adsorption capacity of FZAC is linked to its improved pore network and functionalized surface that promote dye-surface interactions, in agreement with Tran & Nguyen, (2023).

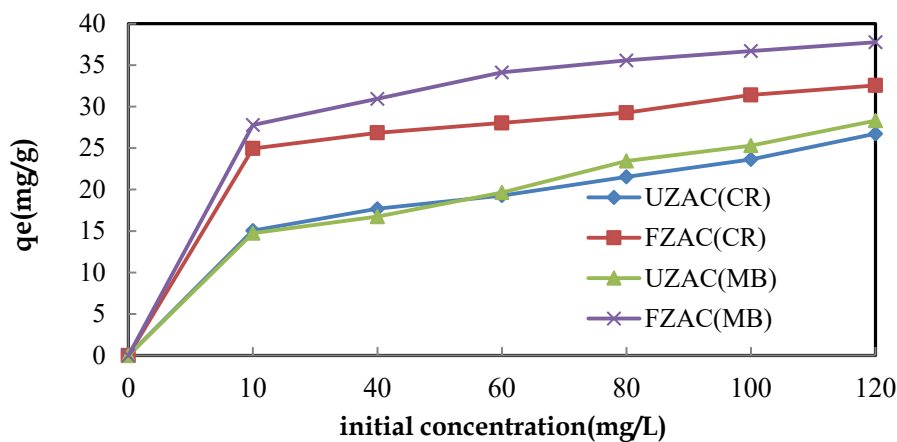


Figure 9: Effect of initial dye concentration on MB and CR adsorption by UZAC and FZAC.

3.3 Adsorption Isotherm Studies

3.3.1 Langmuir isotherm

The Langmuir model was applied to assess monolayer adsorption (Figure 10). The calculated correlation coefficients ($R^2 = 0.675-0.824$) indicate moderate agreement, and the separation factors ($R_L = 0.011-0.769$) suggest favorable adsorption conditions (Ayawei *et al.*, 2017). The highest anticipated adsorption capabilities were 6.33 mg/g (MB) and 7.04 mg/g (CR), confirming that functionalization enhanced adsorption efficiency.

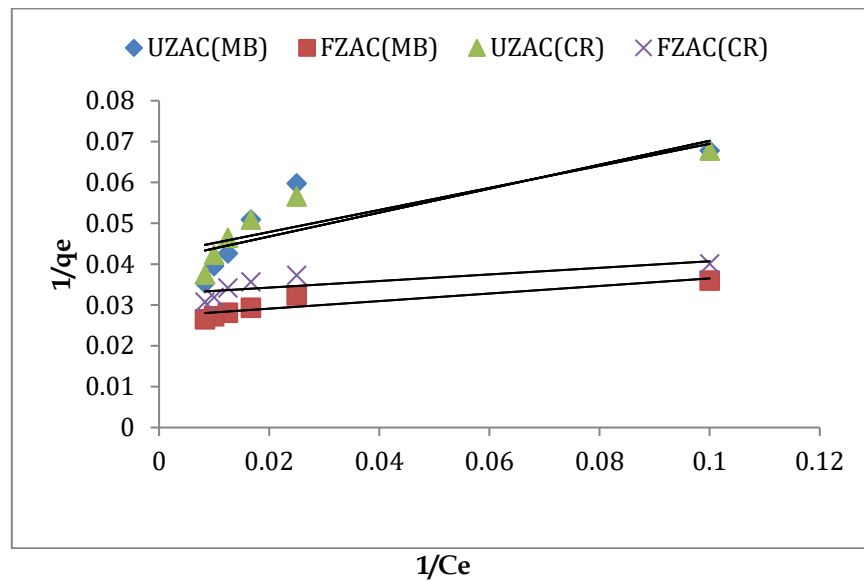


Figure 10: Langmuir adsorption isotherm for MB and CR adsorption.

For UZAC Adsorption/Methylene Blue system

$$\frac{1}{q_e} = 0.04 + 0.292 \frac{1}{C_e} \quad (3)$$

For FZAC Adsorption/Methylene Blue system

$$\frac{1}{q_e} = 0.027 + 0.092 \frac{1}{C_e} \quad (4)$$

For UZAC Adsorption/Congo Red system

$$\frac{1}{q_e} = 0.042 + 0.269 \frac{1}{C_e} \quad (5)$$

For FZAC Adsorption/Congo Red system

$$\frac{1}{q_e} = 0.032 + 0.08 \frac{1}{C_e} \quad (6)$$

3.3.2 Freundlich isotherm

The Freundlich model provided a better fit ($R^2 = 0.851\text{--}0.957$), signifying multilayer adsorption on heterogeneous surfaces (Figure 11). Freundlich constants ($1/n = 0.101\text{--}0.255$) being less than 1 indicate favorable adsorption and strong adsorbent-adsorbate interaction (Benjelloun *et al.*, 2021).

From the graph the following linearized Freundlich adsorption isotherm Equations (8-11) were extracted:

For UZAC Adsorption/Methylene Blue system

$$\ln q_e = 2.018 + 0.255 \ln C_e \quad (8)$$

For FZAC Adsorption/Methylene Blue system

$$\ln q_e = 3.016 + 0.125 \ln C_e \quad (9)$$

For UZAC Adsorption/Congo Red system

$$\ln q_e = 2.127 + 0.221 \ln C_e \quad (10)$$

For FZAC Adsorption/Congo Red system

$$\ln q_e = 2.954 + 0.101 \ln C_e \quad (11)$$

These findings imply that adsorption of MB and CR on UZAC and FZAC occurs on uneven surfaces with varying energy sites, typical of activated carbon materials (Alvarez-Galvan *et al.*, 2022; Mubarik *et al.*, 2023; Wang *et al.*, 2023).

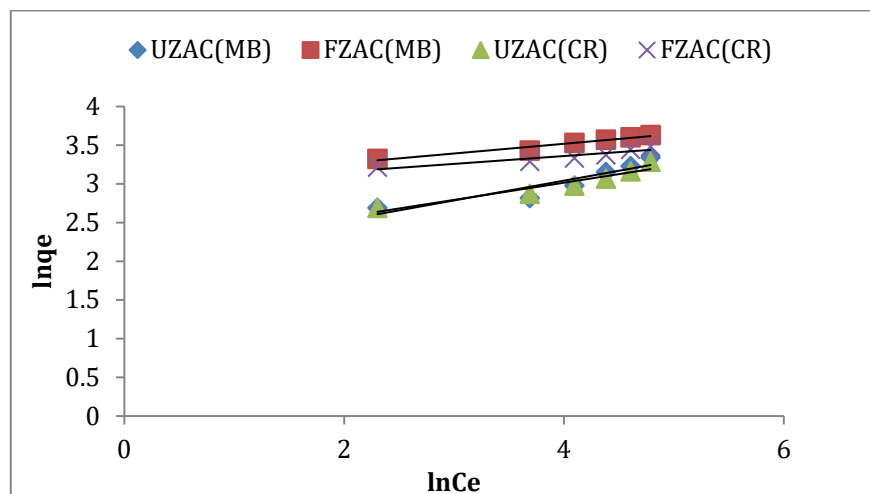


Figure 11: Freundlich adsorption isotherm for MB and CR adsorption.

3.4 Environmental Implications

The ability of nitric acid-functionalized $ZnCl_2$ -activated carbon to eliminate both anionic and cationic dyes demonstrates its adaptability in treating mixed industrial effluents. Its high adsorption rate, substantial surface area, and low preparation cost make it a sustainable choice for wastewater purification. Additionally, utilizing agricultural residues like coconut shells supports circular economy principles and environmental sustainability (Huyen Nguyen & Quoc Le, 2025; Rahman *et al.*, 2024; Van Pho *et al.*, 2025).

4.0 Conclusion

Coconut shell-derived activated carbon produced through zinc chloride activation and subsequent nitric acid modification proved to be an efficient adsorbent for eliminating Methylene Blue and Congo Red dyes from aqueous media. Activation with $ZnCl_2$ significantly enhanced the particular surface area (from $135.55\text{ m}^2/\text{g}$ to $435.98\text{ m}^2/\text{g}$) and increased the pore volume from $0.055\text{ cm}^3/\text{g}$ to $0.154\text{ cm}^3/\text{g}$. Additional treatment with nitric acid further improved the surface characteristics to $810.44\text{ m}^2/\text{g}$ and $0.296\text{ cm}^3/\text{g}$, respectively, leading to a marked rise in adsorption capacity.

The functionalized carbon exhibited amphoteric behavior and achieved rapid adsorption equilibrium within 30 minutes. The adsorption mechanism was primarily governed by electrostatic interactions, complemented by van der Waals forces when surface charge conditions favored attraction. Conversely, electrostatic repulsion at unfavorable pH conditions weakened adsorption forces. Equilibrium data fit both Langmuir and Freundlich isotherms, confirming heterogeneous surface adsorption and favorable dye-adsorbent interaction.

Overall, this research establishes nitric acid-functionalized $ZnCl_2$ -activated carbon from coconut shells as a high-performance, eco-friendly, and low-cost adsorbent for dye removal from wastewater. Its

enhanced porosity, dual dye affinity, and sustainable biomass origin make it a viable candidate for environmental remediation and water purification applications.

References

Ai, L., Zhang, C., & Meng, L. (2011). Adsorption of Methyl Orange from Aqueous Solution on Hydrothermal Synthesized Mg-Al Layered Double Hydroxide. *Journal of Chemical & Engineering Data*, 56(11), 4217-4225. <https://doi.org/10.1021/je200743u>

Alvarez-Galvan, Y., Minofar, B., Futera, Z., Francoeur, M., Jean-Marius, C., Brehm, N., Yacou, C., Jauregui-Haza, U. J., & Gaspard, S. (2022). Adsorption of Hexavalent Chromium Using Activated Carbon Produced from Sargassum ssp.: Comparison between Lab Experiments and Molecular Dynamics Simulations. *Molecules*, 27(18), 6040. <https://doi.org/10.3390/molecules27186040>

Ayawei, N., Ebelegi, A. N., & Wankasi, D. (2017). Modelling and Interpretation of Adsorption Isotherms. *Journal of Chemistry*, 2017, 1-11. <https://doi.org/10.1155/2017/3039817>

Bai R. S. (2001). Biosorption of Cr (VI) from aqueous solution by Rhizopus nigricans. *Bioresource Technology*, 79(1), 73-81. [https://doi.org/10.1016/s0960-8524\(00\)00107-3](https://doi.org/10.1016/s0960-8524(00)00107-3)

Barka, N., Abdennouri, M., El Makhfouk, M., & Qourzal, S. (2013). Biosorption characteristics of cadmium and lead onto eco-friendly dried cactus (*Opuntia ficus indica*) cladodes. *Journal of Environmental Chemical Engineering*, 1(3), 144-149. <https://doi.org/10.1016/j.jece.2013.04.008>

Benjelloun, M., Miyah, Y., Akdemir Evrendilek, G., Zerrouq, F., & Lairini, S. (2021). Recent Advances in Adsorption Kinetic Models: Their Application to Dye Types. *Arabian Journal of Chemistry*, 14(4), 103031. <https://doi.org/10.1016/j.arabjc.2021.103031>

Cayllahua, J. E. B., De Carvalho, R. J., & Torem, M. L. (2009). Evaluation of equilibrium, kinetic and thermodynamic parameters for biosorption of nickel(II) ions onto bacteria strain, *Rhodococcus opacus*. *Minerals Engineering*, 22(15), 1318-1325. <https://doi.org/10.1016/j.mineng.2009.08.003>

Fraile, A., Penche, S., González, F., Blázquez, M. L., Muñoz, J. A., & Ballester, A. (2005). Biosorption of copper, zinc, cadmium and nickel by *Chlorella vulgaris*. *Chemistry and Ecology*, 21(1), 61-75. <https://doi.org/10.1080/02757540512331334933>

Lawal, A. O., Salisu, A. G., Aminu S., Isah, H. H., & Habil, S. K. (2018). Vehicular Emission, VOCs, Diffusive, Air sampler. *American Journal of Environmental Engineering*.

Huyen Nguyen Thi, T., & Quoc Le, H. (2025). Impacts of environmental awareness on enterprise behaviors in Vietnam. *Environmental Economics*, 16(3), 1-13. [https://doi.org/10.21511/ee.16\(3\).2025.01](https://doi.org/10.21511/ee.16(3).2025.01)

Mubarik, S., Ali, S., Manzoor, S., Imran, M., & Ehsan, S. (2023). Decontamination of methylene blue and congo red by SCB/CuO nanocomposites: Isotherms and kinetic studies. *Desalination and Water Treatment*, 307, 212-221. <https://doi.org/10.5004/dwt.2023.29907>

Rahman, Md. M., Saha, S., & Hoque, M. (2024). Unveiling the link between environmental management accounting, energy efficiency, and accountability in state-owned enterprises: An integrated analysis using PLS-SEM and fsQCA. *Environmental Challenges*, 14, 100832. <https://doi.org/10.1016/j.envc.2023.100832>

Tran, H. D., & Nguyen, D. Q. (2023). Study on methylene blue adsorption using cashew nut shell-based activated carbon. *Chimica Techno Acta*, 10(4). <https://doi.org/10.15826/chimtech.2023.10.4.01>

Van Pho, T., Phan, D.-K., Phan, G. Q., & Nguyen, T. T. H. (2025). Impact of financial development, technological innovation, green trade and institutional quality on sustainable development: Revelations from global evidence. *Sustainable Chemistry One World*, 6, 100058. <https://doi.org/10.1016/j.scowo.2025.100058>

Wang, S., Li, W., & Li, G. (2023). Polyethyleneimine modified spent coffee grounds as a novel bio-adsorbent for selective adsorption of anionic Congo red and cationic Methylene blue. *Desalination and Water Treatment*, 290, 147-161. <https://doi.org/10.5004/dwt.2023.29480>

Yakubu, R. O., Yaro, M. N., Habibu, S., & Nasir, S. (2024). Efficient Removal of Congo Red Dye from Aqueous Solution using a Biosorbent derived from *Phoenix Dactylifera* Seeds: Exploring Kinetic and Thermodynamic Parameters.